

## On the Ionian thermohaline properties and circulation in 2010-2013 as measured by Argo floats

Vedrana KOVAČEVIĆ, Laura URSELLA, Miroslav GAČIĆ, Giulio NOTARSTEFANO,  
Milena MENNA, Manuel BENSI and Pierre-Marie POULAIN

*OGS (Istituto Nazionale d Oceanografia e di Geofisica Sperimentale),  
Borgo Grotta Gigante 42/c, Sgonico, Italy*

*\*Corresponding author, e-mail: vkovacevic@ogs.trieste.it*

---

*From all available Argo floats and altimetry data, the surface, intermediate (350 m depth) and deep (1000 m) circulation patterns in the Ionian Sea were analysed in detail for four consecutive years (2010, 2011, 2012 and 2013). In addition, thermohaline properties from float measurements were described and compared considering among all, the Dense Water Overflow from the Adriatic, particularly the one due to the strong winter air-sea heat loss in 2012. In the flow field, energetic closed circulation structures with the spatial scale of about 100 km were present during the entire study period. More specifically, the Pelops Gyre is observed from the surface down to more than 1000 m depth. A multi-lobe anticyclonic feature in the centre of the Ionian basin located to the north of the Mid Ionian Jet was also well evident in the same depth interval. The sub-basin-wide cyclonic circulation in the northern Ionian was clearly documented only in the close vicinity of the basin flanks at all the three levels. The most prominent signal of the Adriatic Dense Water (AdDW) was evidenced at about 1000 m depth in the northwestern portion of the basin in late spring 2012. Afterwards, very likely the AdDW progressively sank along its way southward and its signal was not recorded anymore because of the limited range of the float profiles (max 2000 m).*

---

**Key words:** Ionian Sea, buoyancy floats, surface topography, sub-basin variability, inter-annual variability

### INTRODUCTION

The Ionian Sea as a part of the Adriatic – Ionian Bimodal Oscillating System (BiOS) represents a key area of the Mediterranean Sea (Fig. 1). Its influence on the overturning circulation and dense water formation processes regulates the long-term variability of both the Eastern and Western Mediterranean (GAČIĆ *et al.*, 2011; GAČIĆ *et al.*, 2013). The Ionian Sea circulation, due to the internal feedback with the Adriatic, varies on almost decadal scale pass-

ing from cyclonic to anticyclonic modes and vice versa (BESSIERES *et al.*, 2013 and references cited therein). The horizontal circulation modes have been detected and observed mainly from altimetric measurements (LARNICOL *et al.*, 2002; VIGO *et al.*, 2005) while some considerations on the vertical structure of the Ionian circulation have been done only recently using float and oceanographic campaign data (GAČIĆ *et al.*, 2014). Specifically, GAČIĆ *et al.* (2014) have shown that the Ionian behaves as a two-layer fluid and that decadal inversions as well as anomalous revers-

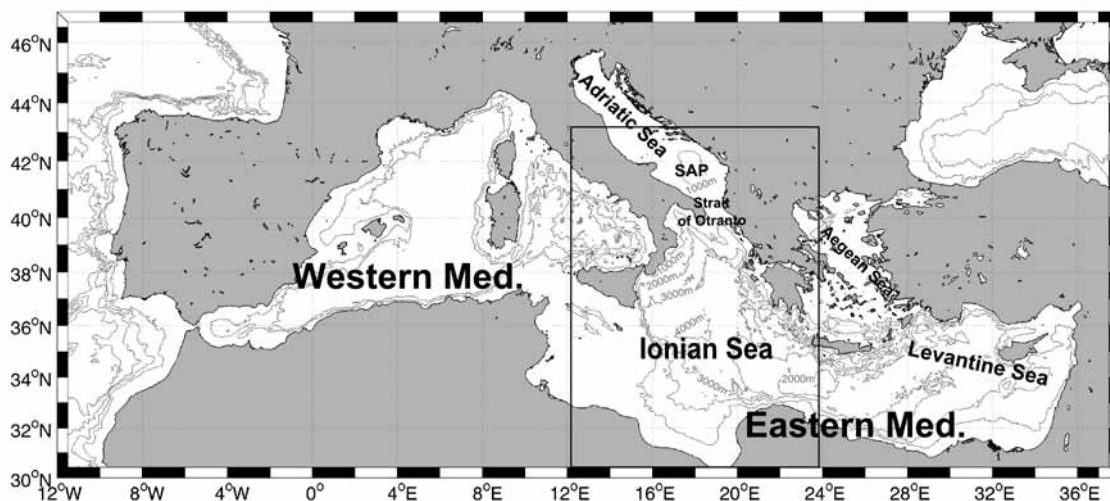


Fig. 1. Map of the Mediterranean Sea. Thin-line rectangle indicates the study area

als of the North Ionian Gyre (NIG) are generated by the spreading of the bottom water formed in the Adriatic Sea (AdDW) or, during the Eastern Mediterranean Transient (EMT), in the Aegean Sea. This water of density varying on interannual and decadal scales changes the horizontal pressure gradient, inverting the horizontal circulation (GAČIĆ *et al.*, 2010). On one hand, the presence of the cyclonic or anticyclonic NIG affects the thermohaline and biochemical properties of the water mass advected through the Strait of Otranto and thus the biogeochemical properties of the entire Adriatic. On the other hand, winter climatic conditions over the Adriatic as well as the buoyancy of the water column (salinity in the southern Adriatic deep-water formation area) determine the density of the AdDW affecting the NIG circulation. The circulation pattern in the Ionian also determines the spreading pathways of the Atlantic Water, the stronger/weaker dilution of the Levantine/Adriatic Seas, and the preconditioning for the winter convection in the two Mediterranean sub-basins. It has also been evidenced that the preconditioning for the Western Mediterranean Dense Water formation depends on the Ionian circulation mode (GAČIĆ *et al.*, 2013), which determines the amount and characteristics of the Levantine water that spreads in the Western Mediterranean. Very recent results suggest that the time scale of the NIG inversion can become appreciably shorter

due to strong winter air-sea heat fluxes over the Adriatic dense water formation site such as during the strong winter 2012 (GAČIĆ *et al.*, 2014). This “premature” inversion was caused by the formation of very dense Adriatic waters, flowing along the Ionian continental slope in May and inverting the bottom pressure gradient.

The aim of this work is to describe in detail the pattern of the horizontal spreading of the different water masses entering the Ionian Sea in the specific period 2010-2013 when the “premature” reversal of the Ionian basin-wide circulation took place. The research is based on Argo temperature-salinity data, which cover rather well the studied area. The sub-surface thermohaline properties are interpreted and compared with the surface altimetric data and geostrophic flow.

The data and methods are described in section 2. In section 3 we report the dynamic structures and the main thermohaline features in the upper 1000 m during the four years. In section 4 we discuss more in detail the differences in thermohaline properties observed in 2012 and 2013 and finally, in section 5, the main conclusions of our investigations are given.

## DATA AND METHODS

The Argo profiling floats used for this work provided data in the period 1/1/2010-

31/12/2013. They were deployed in the framework of the Argo program in the Mediterranean Sea (MedArgo, see POULAIN *et al.*, 2007). The profilers are equipped with Sea-Bird CTD (Conductivity-Temperature-Depth) sensors (models SBE 41 or 41CP) with accuracies of  $\pm 0.002^\circ \text{C}$ ,  $\pm 0.002 \text{ PSU}$  and  $\pm 2 \text{ dbar}$  for temperature (T), salinity (S), and pressure (P), respectively (as reported on the Seabird web site: [http://www.seabird.com/products/spec\\_sheets/41data.htm](http://www.seabird.com/products/spec_sheets/41data.htm)). The Argo floats were programmed with a cycle length between 4 and 10 days and a maximal profiling depth between 1000 and 2000 dbar (OGS web page dedicated to MedArgo <http://nettuno.ogs.trieste.it/sire/medargo/active/index.php>; Coriolis web page: <http://www.coriolis.eu.org/>). The sampling depth is variable but it is generally as follows: in the upper layer, it is set to 5 dbar in the interval [0 100 dbar]; 10 dbar in the interval [100 700], while below, in the interval [700 2000], it is set to 50 dbar, and anyhow including the near bottom values. However, the sampling resolution is increased in the most recent float models. The parking-drifting depth is set at 350 m, except for the three floats released in April 2012 that drifted at 1000 m depth, and profiled down to a maximum depth of 1180 m. The quantity of the floats that we take into consideration in this study is 7 in 2010, 8 in 2011, 16 in 2012 and 20 in 2013. We individuate the floats using their WMO (World Meteorological Organization) numbers.

The data were processed and quality-controlled using standard tests at Argo Data Assembly Centre (DAC). A delayed-mode quality control of P, T and S data was then applied in accordance to the ARGO QUALITY CONTROL MANUAL (2013), and in particular the Owens-Wong method was adopted (OWENS & WONG, 2009) to check the S data. The Argo float S profiles were also qualitatively compared to a reference dataset (for the methods refer to NOTARSTEFANO & POULAIN, 2008); this comparison detected no drift of the conductivity sensor, while it highlighted a negative offset (0.0151 PSU) in the S data for the Argo float 6900952 (NOTARSTEFANO & POULAIN, 2013), which was corrected. After removing the spikes, the potential drifts or offsets of

the temperature and conductivity sensors were detected to be smaller than the natural variability of the water column and hence no delayed mode correction was deemed necessary. Potential temperature ( $\theta$ ) and potential density anomaly ( $\sigma_\theta$ ), with reference pressure equal to 0 dbar were calculated.

The altimetry data used for this study are gridded ( $1/8^\circ$  Mercator projection grid) Ssalto/Duacs weekly, multi-mission, delayed time (quality controlled) products from AVISO (SSALTO/DUACS users handbook 2013). Among the available versions of the delayed time products we have selected the reference data series, based on two satellites (Jason-2 / Envisat or Jason-1 / Envisat or Topex/Poseidon / ERS) with the same groundtrack. These data series are homogeneous all along the available time period, thanks to a stable sampling. The Absolute Dynamic Topography (ADT, in cm) were downloaded. The ADT is the sum of sea level anomaly and Synthetic Mean Dynamic Topography, estimated by RIO *et al.* (2007) over the 1993-1999 period.

Maps of annual ADT averages over the Ionian Sea for the 2010-2013 period (Fig. 2) are superimposed with float trajectories at 350 m in order to describe the main similarities and differences between the surface and intermediate currents.

## Dynamics and thermohaline properties at different depths

### Surface layer

The absolute geostrophic currents can be derived from the ADT and the highs and lows in ADT (Fig. 2) correspond to anticyclonic and cyclonic gyres, respectively.

The ADT mean yearly maps (Fig. 2) corroborate the principal dynamic features of the upper thermocline circulation pattern of the Ionian basin which mainly consists of meandering currents and permanent, semi-permanent and transient gyres, both cyclonic and anticyclonic (MALANOTTE-RIZZOLI *et al.*, 1997). The gyres are either single or multi-lobe structures. Their diameters are about 100-200 km, and, as shown

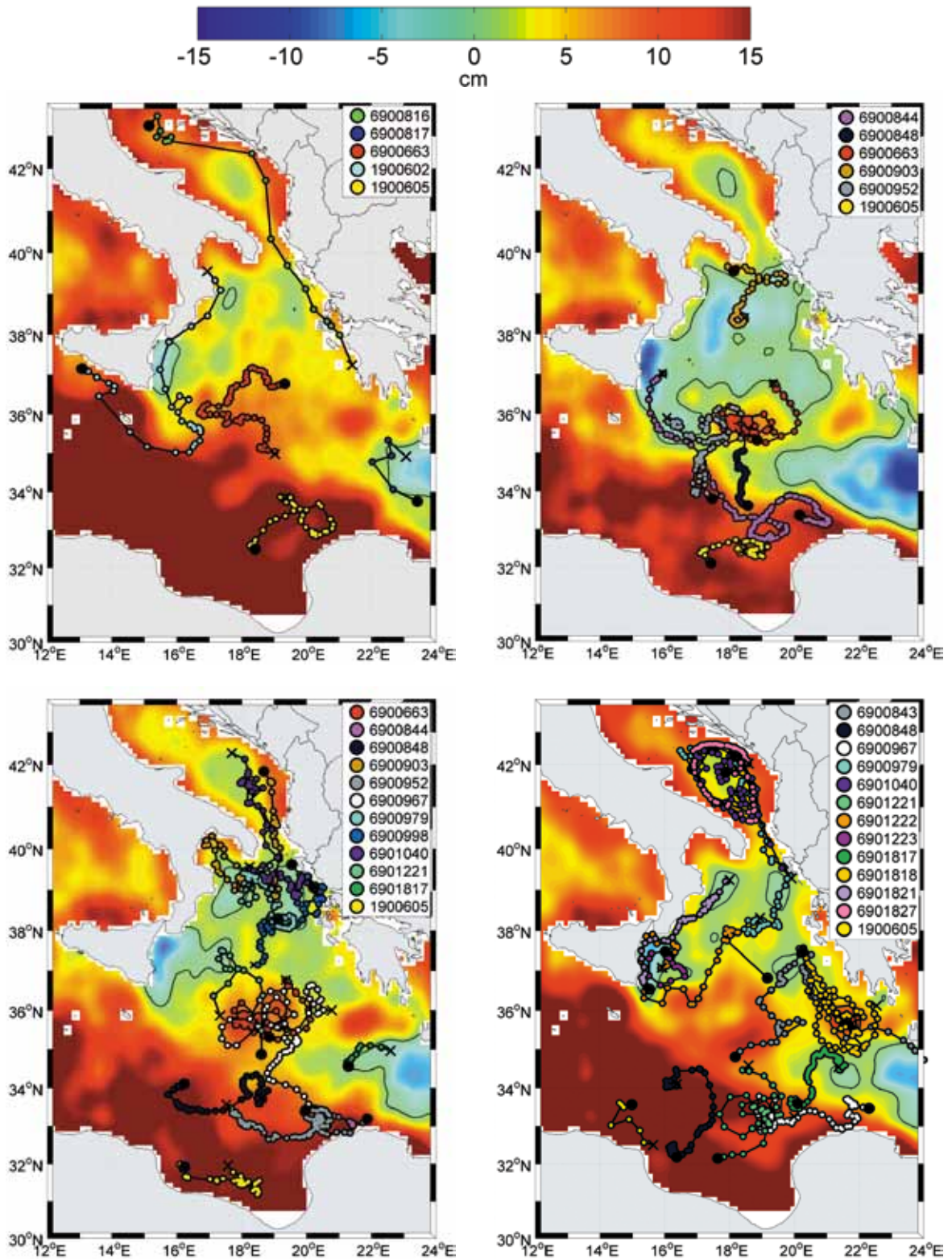


Fig. 2. ADT annual mean maps in 2010 (a), 2011 (b), 2012 (c) and 2013 (d). Superimposed trajectories at 350 m of the selected floats are color-coded. Black crosses (dots) denote the initial (final) position. Black solid line delineates the zero contour of the sea level

by NITTIS *et al.* (1993), they are usually several times larger than the first internal Rossby radius of deformation ( $R_i$ ).  $R_i$  is a typical horizontal length scale (defined as wavelength over  $2\pi$ , as in EMERY *et al.*, 1984) that depends on the stratification and at which the Earth rotation effects become as important as gravitational ones. It characterizes the meso-scale dynamics, i. e. eddies, and in the Ionian Sea, it is between 9 and 14 km large (NITTIS *et al.*; 1993, GRILLI & PINARDI, 1998). The northern Ionian Sea is characterized prevalently by cyclonic structures, the central and southern Ionian by anticyclonic ones. The location and the extension of the cyclonic and anticyclonic features vary in the course of the years. Some of the anticyclones are of long duration, such as the Pelops anticyclone and central Ionian anticyclone (ROBINSON *et al.*, 1991; NITTIS *et al.*, 1993; MALANOTTE-RIZZOLI *et al.*, 1997; ROBINSON *et al.*, 2001).

The footprints of the gyres are observed throughout the studied period (Fig. 2), and their influence protrudes down to deeper layers. The Pelops anticyclone is located on the eastern side of the Ionian (21-22°E, 36°N). The central Ionian anticyclone (18-20°E, 35-37°N) is frequently observed above the deepest Ionian trough (> 4000 m). Moreover, a pool of several cyclones persists in the northern Ionian (in the zone between 36 and 40°N). In 2011, the area influenced by cyclonic structures was wider than in 2010, 2012, or 2013. The sub-basin scale pattern in the northern Ionian can be summarized as prevalently anticyclonic in 2010 and prominently cyclonic in 2011. The cyclonic circulation weakens in 2012, while in 2013 the anticyclonic meander widens and strengthens retreating slightly southward. These variations are part of the basin-scale BiOS inversion cycle (GAČIĆ *et al.*, 2014).

### Intermediate layer (350 m depth)

The float parking depths at 350 m were used to track pathways of the intermediate waters (mainly the Levantine Intermediate Waters, LIW). The circulation features observed from the float trajectories suggest that it is hard to

discern the large-scale sub-basin steady flow from the flow influenced by the cyclones, anticyclones and meanders. These characteristics of the surface circulation are generally reiterated also in the intermediate layer. A relatively steady flow prevails only along the periphery of the north-western and western Ionian (Figs. 2a and 2d) where the southward stream follows the bathymetric contours of the slope. In contrast, a relatively fast northward flow appears along the eastern flank (Figs. 2a, 2c and 2d). However, most floats feel the influence of the cyclones and anticyclones. In particular, the following floats illustrate this: 6900663 and 6900952 in Figs. 2b and 2c, 6901221 and 6900967 in Figs. 2c and 2d, and 6901040, 6901223 and 6901818 in Fig. 2d. The floats which travel around the western periphery may exit the Ionian through the Sicily Channel (in 2010, Fig. 2a), or reach its southern portion (in 2011, Fig. 2b). Some deviate toward the centre and then northward, like in 2013 (Fig. 2d). In the southern Adriatic, the floats recirculate within the sub-basin scale cyclone (Figs. 2a and 2d), with a mean speed of  $\sim 6$  cm/s, and sometimes get trapped by the smaller mesoscale eddies in the centre of the Southern Adriatic Pit (SAP). The float 6901040, released in the Southern Adriatic in March 2012 (Fig. 2c), entered the northern Ionian during August 2012 along the western flank of the Strait of Otranto. Then it crossed the northern Ionian meandering toward the eastern flank and returned into the southern Adriatic during January 2013, where it has still been drifting at the end of 2013 (Fig. 2d).

In the south, the float trajectories follow the eastward meandering Mid Ionian Jet (MIJ). Floats 6900844 in Fig. 2b, 6900844, 6900952 and 6900967 in Fig. 2c and 6900967 in Fig. 2d corroborate this. For some time they can be trapped by cyclonic and anticyclonic gyres (Fig. 2a, float 1900605; Fig. 2b floats 6900844 and 1900605; Fig. 2c floats 6900848 and 6900952; Fig. 2d, float 6900979) generated by the instability of the current (Libyan eddies described by HAMAD *et al.*, 2006 and MILLOT & TAUPIER-LETAGE, 2005). The float trajectories depict the Ionian anticyclone in the centre of the basin (Fig. 2a, float 6900663; Fig. 2b, floats 6900663 and

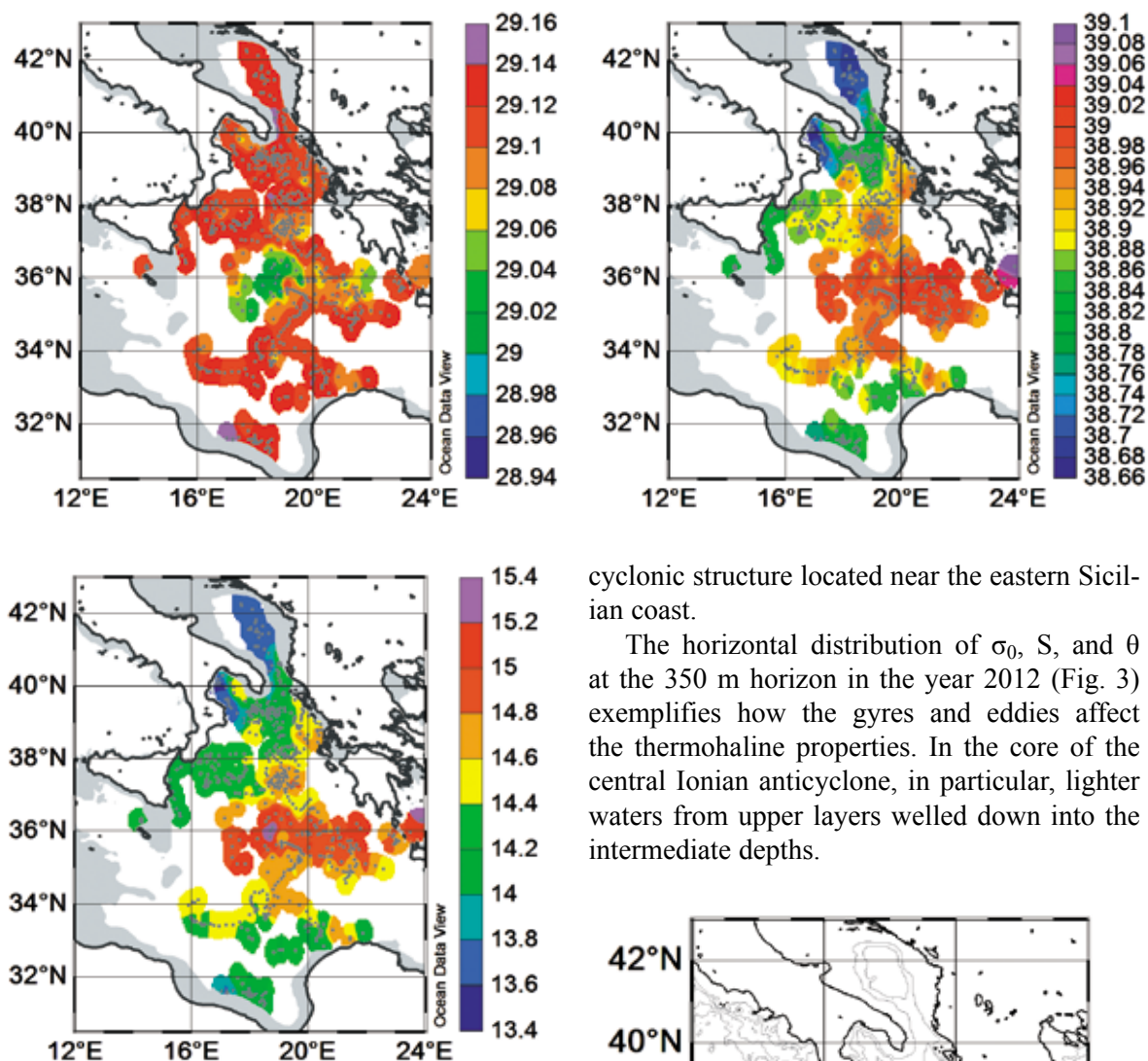


Fig. 3. Horizontal distribution of  $\sigma_\theta$ ,  $\text{kgm}^{-3}$  (a),  $S$  (b), and  $\theta$ ,  $^\circ\text{C}$  (c) at 350 m in 2012

6900952; Fig. 2c, floats 6900663 and 6900967) and the Pelops Gyre (Fig. 2d; float 6901818) in its eastern portion. To the south of the MIJ floats show prevalent anticyclonic circulation and consequently a westward current close to the Libyan coast (MENNA & POULAIN *et al.*, 2010).

In the north, floats deployed on the eastern flank of the Ionian follow the inflow of the LIW into the Adriatic Sea (Fig. 2a, float 6900816; Fig. 2d, floats 6900979 and 6901040), whereas those deployed on the western flank (floats 6901222 and 6901223 in Fig. 2d) describe the

cyclonic structure located near the eastern Sicilian coast.

The horizontal distribution of  $\sigma_\theta$ ,  $S$ , and  $\theta$  at the 350 m horizon in the year 2012 (Fig. 3) exemplifies how the gyres and eddies affect the thermohaline properties. In the core of the central Ionian anticyclone, in particular, lighter waters from upper layers welled down into the intermediate depths.

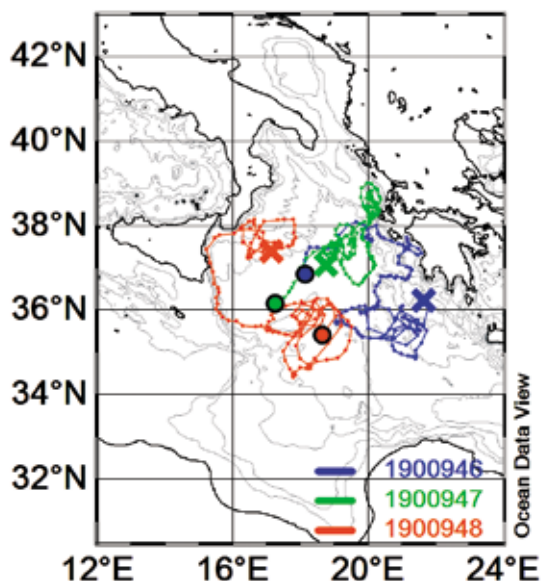


Fig. 4. Trajectories of the three floats drifting at 1000 m depth during the 2012-2013 interval. Crosses indicate the location of deployment in April 2012, and large dots the last location in 2013. Isobaths 500, 1000, 2000, 3000, and 4000 m are depicted

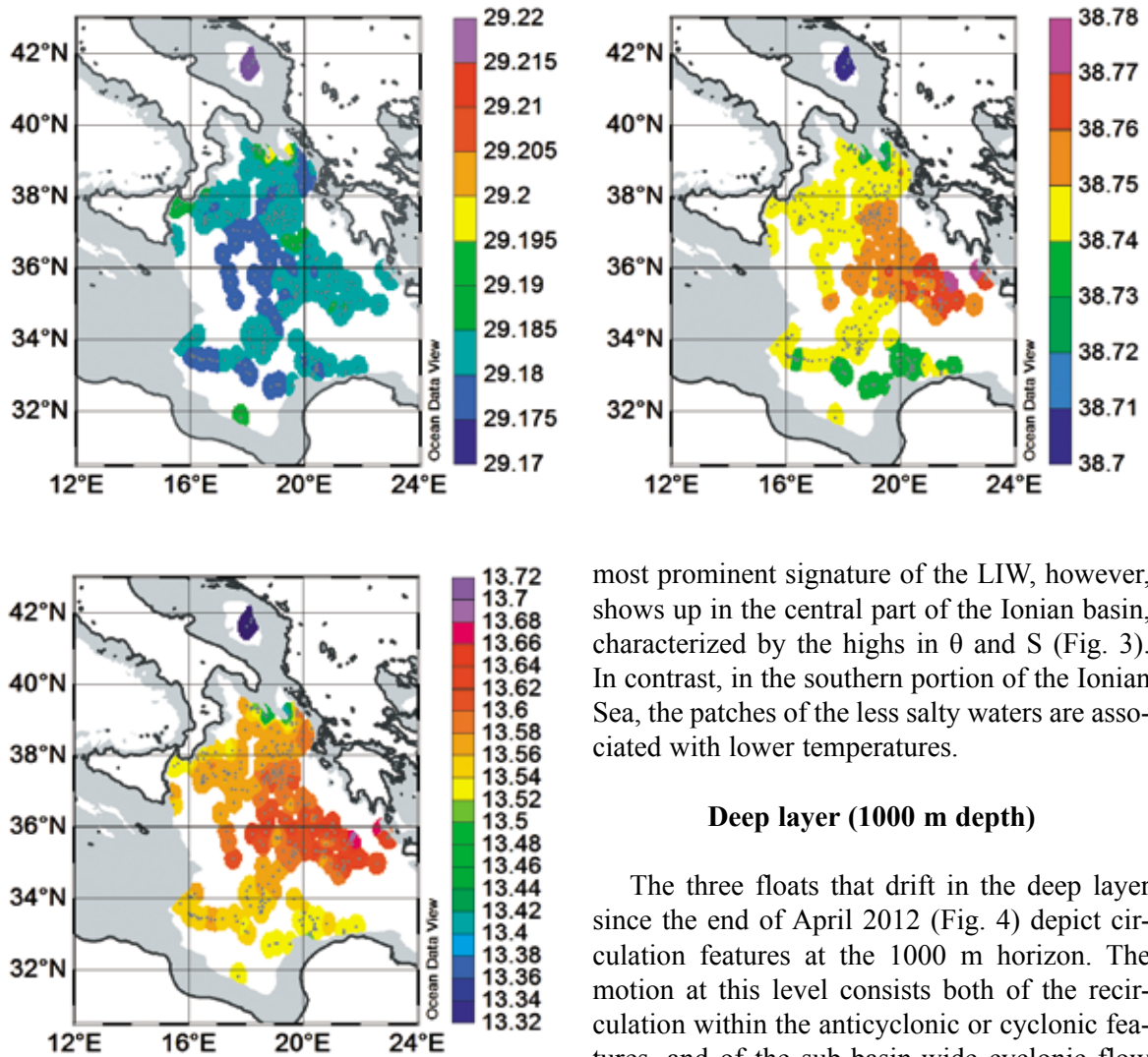


Fig. 5. Horizontal distribution at 1160 m in 2012:  $\sigma_0$ ,  $\text{kgm}^{-3}$  (a),  $S$  (b), and  $\theta$ ,  $^{\circ}\text{C}$  (c). The dark violet colour out of scale in (a) corresponds to the  $\sigma_0$  range 29.27-29.28. The dark blue colour in (b) corresponds to the  $S$  range 38.699-38.771, while in (c) it corresponds to the  $\theta$  range 12.95-12.96

In the northern Ionian, near the Strait of Otranto, there is a restricted area with pronounced horizontal gradient in  $S$  and  $\theta$ . There are saltier and warmer waters along the eastern flank, and diverse, less salty and cooler waters in the middle of the Strait, as shown by  $S$  and  $\theta$  in Fig. 3. Indeed, while the LIW inflows into the Adriatic, modified intermediate waters outflow from the southern Adriatic basin. The

most prominent signature of the LIW, however, shows up in the central part of the Ionian basin, characterized by the highs in  $\theta$  and  $S$  (Fig. 3). In contrast, in the southern portion of the Ionian Sea, the patches of the less salty waters are associated with lower temperatures.

#### Deep layer (1000 m depth)

The three floats that drift in the deep layer since the end of April 2012 (Fig. 4) depict circulation features at the 1000 m horizon. The motion at this level consists both of the recirculation within the anticyclonic or cyclonic features, and of the sub-basin-wide cyclonic flow along the isobaths. The float 1900948 deployed on the northwestern Ionian slope, first circulated within an anticyclone centred at  $37.5^{\circ}\text{N}$ , and afterwards continued southward along the isobaths. At  $35.5^{\circ}\text{N}$  it turned toward the centre of the Ionian and recirculated first cyclonically and then anti-cyclonically in the region of the surface Central Ionian anticyclone ( $18\text{-}20^{\circ}\text{E}$ ,  $34.5\text{-}36^{\circ}\text{N}$ , Fig. 4).

The float 1900946, released in the eastern part of the Ionian Sea, first turned anticyclonically (probably due to the deep Pelops anticyclone), moved into the centre of the Ionian describing a series of meanders, and then turned cyclonically toward the northeastern Ionian flank. By the end of the 2013 its position was close to the starting location of the float 1900947 released in the cen-

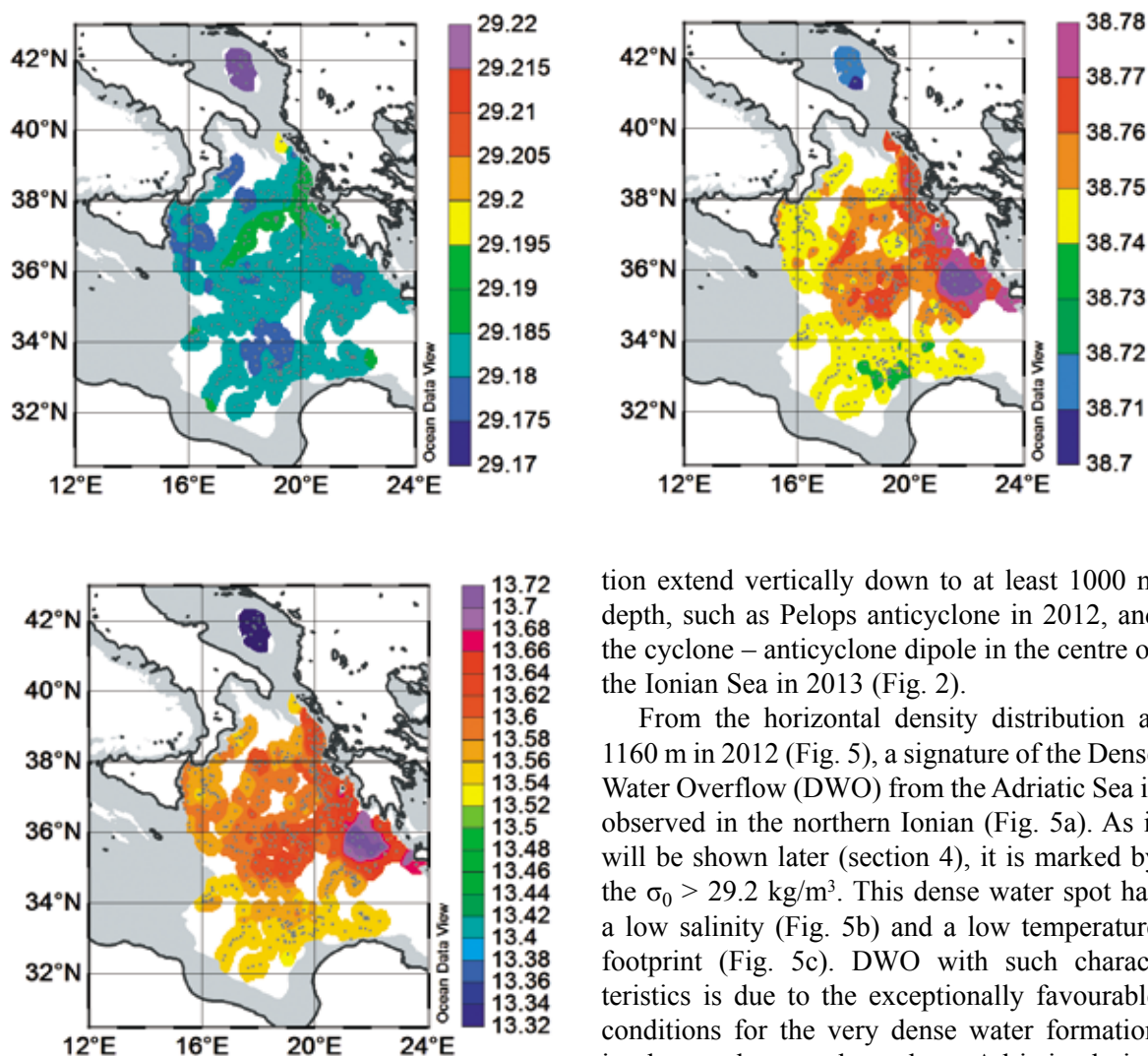


Fig. 6. Horizontal distribution at 1140 m in 2013:  $\sigma_0$ ,  $\text{kgm}^{-3}$  (a),  $S$  (b), and  $\theta$ ,  $^{\circ}\text{C}$  (c). The violet colour out of scale in (a) corresponds to the  $\sigma_0$  range 29.27-29.28. The dark blue colour in (c) corresponds to the  $\theta$  range 13.02-13.05

tre of the Ionian. The float 1900947 performed a number of anticyclonic and cyclonic turnings between the centre of the Ionian and the Greek continental slope. By the end of 2013, it came close to the deepest central Ionian pit.

From our data, one could thus conclude that in the second part of 2012 and 2013 the general sub-basin deep circulation at 1000 m level in the northern Ionian was mainly cyclonic (Fig. 4). In addition, prominent cyclonic or anticyclonic gyres embedded in this sub-basin scale circula-

tion extend vertically down to at least 1000 m depth, such as Pelops anticyclone in 2012, and the cyclone – anticyclone dipole in the centre of the Ionian Sea in 2013 (Fig. 2).

From the horizontal density distribution at 1160 m in 2012 (Fig. 5), a signature of the Dense Water Overflow (DWO) from the Adriatic Sea is observed in the northern Ionian (Fig. 5a). As it will be shown later (section 4), it is marked by the  $\sigma_0 > 29.2 \text{ kg/m}^3$ . This dense water spot has a low salinity (Fig. 5b) and a low temperature footprint (Fig. 5c). DWO with such characteristics is due to the exceptionally favourable conditions for the very dense water formation in the northern and southern Adriatic during winter 2012 (MIHANOVIĆ *et al.*, 2013; BENSI *et al.*, 2013a; GAČIĆ *et al.*, 2014). From the available float data in 2013 at the nearly same horizon, there is no such a marked DWO signature (Fig. 6). We hypothesize that the 2012 AdDW sunk into deeper layers of the Ionian Sea and it was not detectable any more the following year because the vertical profiles did not reach depths larger than 2000 m.

The float movements at 1000 m depth show (Fig. 4) that the deep circulation can be fast enough to affect the deep-water properties distribution, their exchange and mixing across a wider area of the Ionian Sea in a relatively short period (within only a year or two).



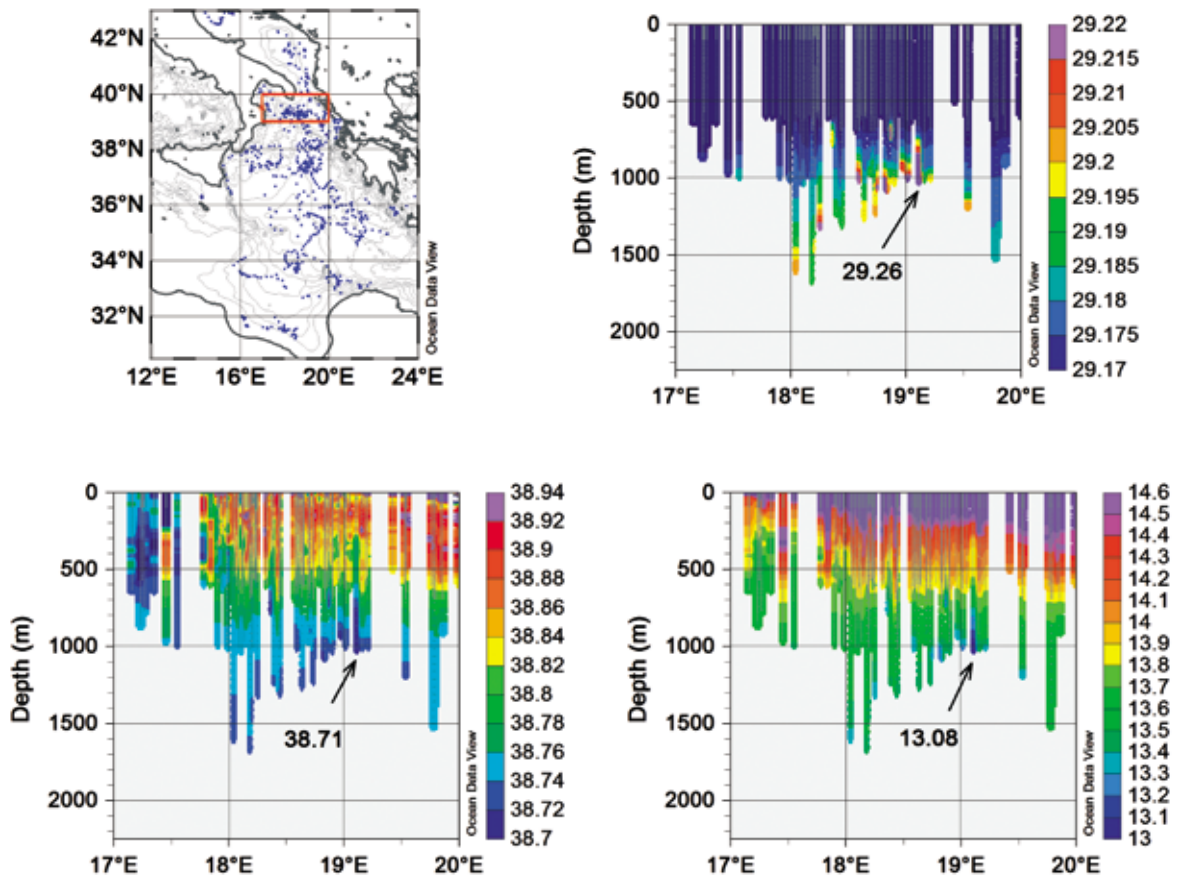


Fig. 7. Area of the zonal section  $1^{\circ}\text{N}$  large and centred at  $39.5^{\circ}\text{N}$  (red) in 2012; float surface positions are indicated by black dots (a). Vertical distribution within the zonal section  $39.5^{\circ}\text{N}$  in the layer 100-2000 m of:  $\sigma_0$ ,  $\text{kg-m}^{-3}$  (b),  $S$  (c), and  $\theta$ ,  $^{\circ}\text{C}$  (d); the profiles are indicated by grey dots

### Thermohaline properties during 2012 and 2013

To localize the DWO event of 2012 in time and space, we depict the vertical distribution of the thermohaline properties by means of the composite zonal sections, taking into account all the float data found each year, 2012 and 2013, within limited areas in the northern Ionian (Fig. 7a).

The depth-longitude diagrams in Figs. 7b, 7c, and 7d illustrate the pseudo section of Fig. 7a located in the northernmost part of the Ionian Sea. This area is of particular interest because there we observed the Adriatic DWO in 2012 and we are confident that for most of this section, the float profiles have reached the bottom, and hence, they provide useful information about thermohaline properties of the bottom

layer. The vertical distribution is in fact a space-time composite, provided by the profiles of the four floats that crossed the section during 2012, but not simultaneously. The densest core ( $\sigma_0 = 29.26 \text{ kg/m}^3$ ) corresponds to a relatively cold ( $\theta = 13.08^{\circ}\text{C}$ ) and fresh ( $S = 38.71$ ) deep water at around  $19.1^{\circ}\text{E}$ . This plot shows also that the dense water signature seems to deepen and spread prevalently westward of  $19^{\circ}\text{E}$ .

Dense water blobs illustrate, on the one side, the impulsive and disconnected nature of the DWO spreading. On the other side, they can also reflect a discontinuing spatial and temporal nature of the measurements conducted by the floats, which move and sample the DWO signal in a spotty (irregular) way. As to the nature of the DWO veins, they discharge out from the Strait of Otranto in different moments, and at different depths, depending on the density of the

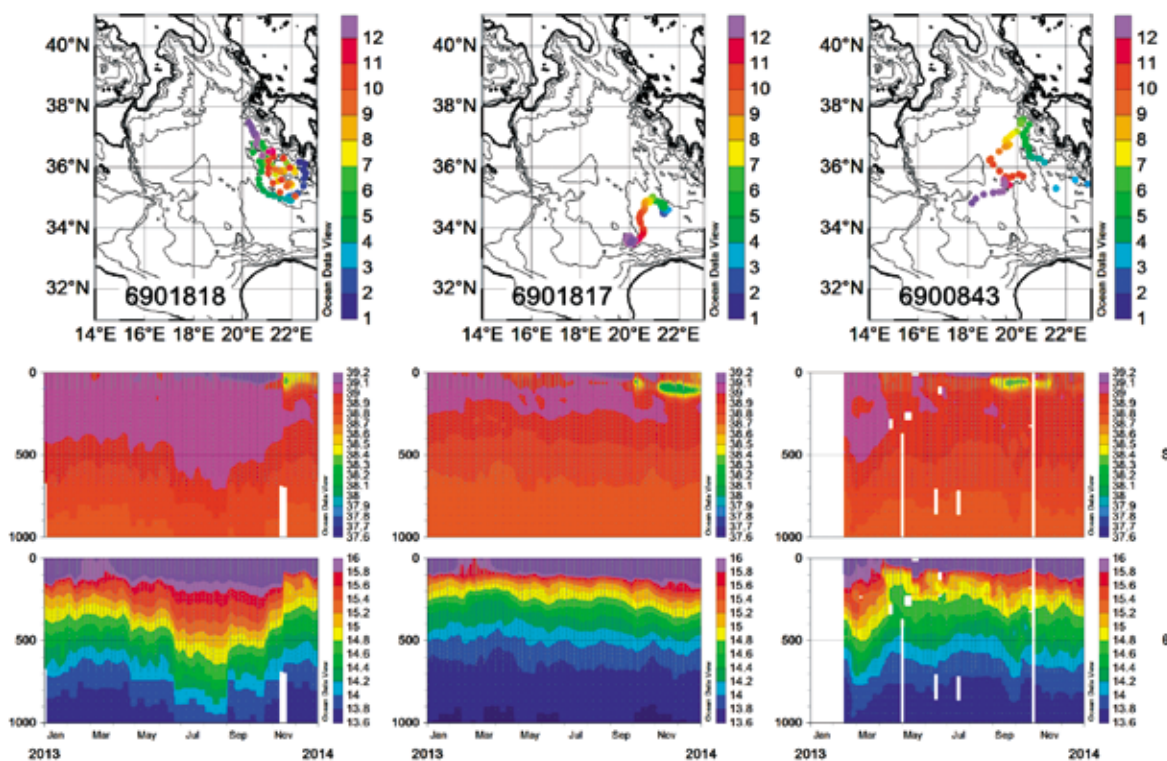


Fig. 8. Month-depth diagram depicting the time evolution of  $S$  and  $\theta$  ( $^{\circ}\text{C}$ ) from some of the profiles carried out in the eastern (a), southeastern (b) and central Ionian (c) during 2013 in the upper 1000 m. Top: colour scale of the float trajectory indicates the month of the year

waters involved in the discharge. URSELLA *et al.* (2011) studied the DWO variability at the inlet of the Strait of Otranto and they ascertained that the DWO temporal and spatial variability are often connected and influenced by the deep mesoscale eddies. From the single float profiles (not shown) we observed the timing of the DWO discharge at various depths and sites. The highest bottom-layer densities with  $\sigma_0 \sim 29.23 \text{ kg/m}^3$ , at around  $19^{\circ}\text{E}$  (Fig. 7b) were captured from July to August 2012, while the maximum single point  $\sigma_0$  value at the Strait of Otranto was  $29.26 \text{ kg/m}^3$  measured at the end of July. This highlights the process of mixing that affects the AdDW during its way towards the abyssal Ionian. A density of  $29.26 \text{ kg/m}^3$ , for the DWO is exceptional if compared with the values observed at the Strait of Otranto in the previous years (BENSI *et al.*, 2013a). Therefore, we were interested in exploring the evolution of the thermohaline conditions also in 2013. For this purpose, our first approach was to compare the vertical thermohaline distri-

butions between 2012 and 2013 over the same area. However, the presence of the floats within the  $39.5^{\circ}\text{N}$  section was too scarce in 2013, with respect to 2012. The southern section at approximately  $38.5^{\circ}\text{N}$  (Fig. 7a) seemed to be more appropriate for such a comparison, as far as the data coverage is concerned. In this area, however, the bottom depths are larger than the maximum level reached by the float profiles (2000 m), and therefore we miss the information about the deepest layer characteristics, where the densest waters lie. The view of the entire water column is available only on the flanks of the section, where the bottom depth is less than 2000 m. We have found out that the prominent 2012 DWO signal captured at  $39.5^{\circ}\text{N}$  is absent in both 2012 and 2013 at the southern section centred at  $38.5^{\circ}\text{N}$  (not shown). One possible reason is that the DWO signal might have been smoothed due to interpolation over time and space, or, more probably, that the densest waters have been spreading at greater depths, below

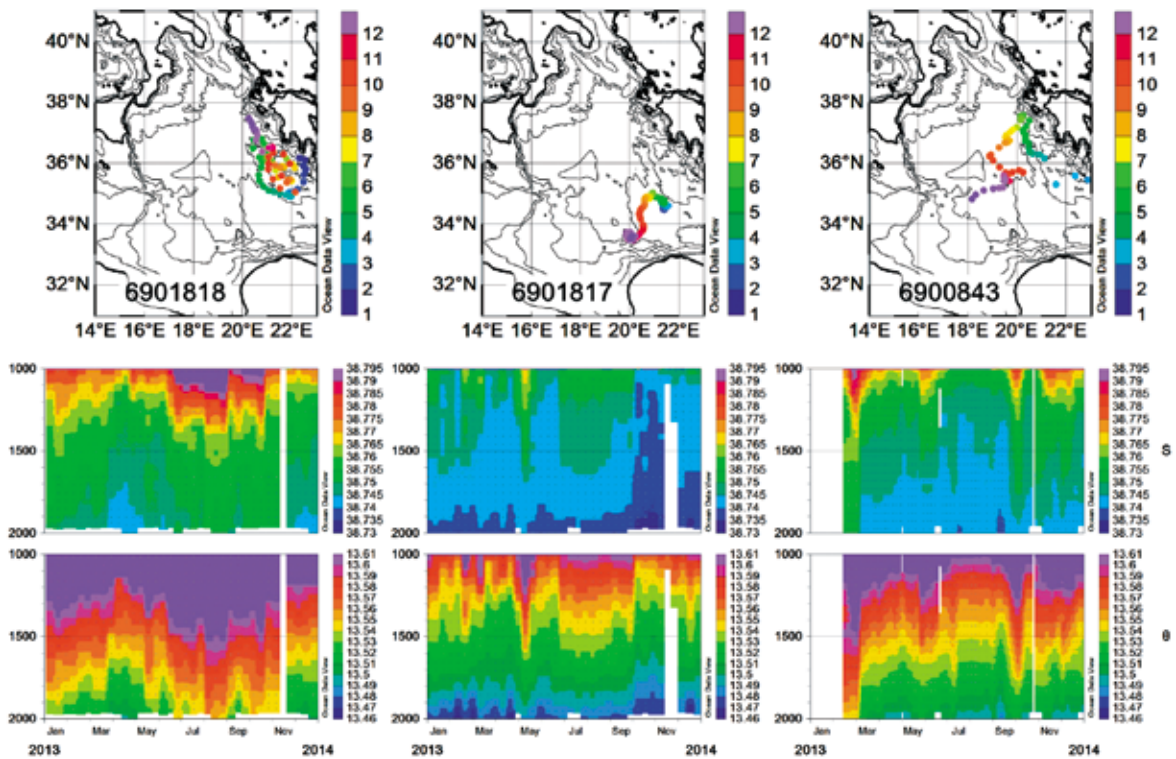


Fig. 9. Month-depth diagram depicting the time evolution of  $S$  and  $\theta$  ( $^{\circ}\text{C}$ ) from some of the profiles carried out in the eastern (a), southeastern (b) and central (c) Ionian during 2013 in the layer between 1000 and 2000 m. Top: colour scale of the float trajectory indicates the month of the year

2000 m, and their signal was out of reach for the float profiles.

Therefore, to better understand and describe the dynamics and the water properties, which may be masked in the yearly map of 2013, we analysed few selected single float depth/time sections. The most significant floats travelling in the Ionian Sea have been chosen for this purpose. In particular, floats 6901818, 6901817 and 6900843 are located in the eastern, southeastern and central parts of the basin (Figs. 8 and 9). Floats 6901821, 6901222 and 6900979 cover the northern and northwestern areas (Figs. 10 and 11). Float 6901221 travels in the southern portion (Fig. 12). We focus solely on the salinity and temperature characteristics, because the signal of dense waters was not evident in the available density profiles. The description will focus on the upper layer (0-1000 m) and the lower layer (1000-2000 m), separately.

In the eastern Ionian Sea we observe the signature of the fresher Atlantic Waters (AW,  $S <$

38.4) at depths  $< 100$  m for all the three floats (Fig. 8), but at different times, corresponding to different locations. Along the Greek coast (the southeastern Ionian, Fig. 8a) there is a clear evidence of waters of low salinity from November on, i.e. along the northernmost part of the track, out of the Pelops gyre. For the remaining part of the year/track, the upper layers, down to 500 m and down to 700-800 m within the gyre, have characteristics of saltier and warmer waters, probably of both Aegean and Levantine origin. The AW is also visible during October-November in the southeastern part of the basin (Fig. 8b), south of  $34^{\circ}\text{N}$ , associated with the eastward transport by the MIJ. The uppermost layer in the central part of the Ionian shows again the presence of the AW to the east of the deepest pit during September-October (Fig. 8c).

Fig. 9 illustrates the eastern deep portion of the Ionian basin, limited to the 1000-2000 m layer. Float 6901818 (Fig. 9a) passed through the saline ( $S \sim 38.76$ ) and relatively warm ( $\theta$

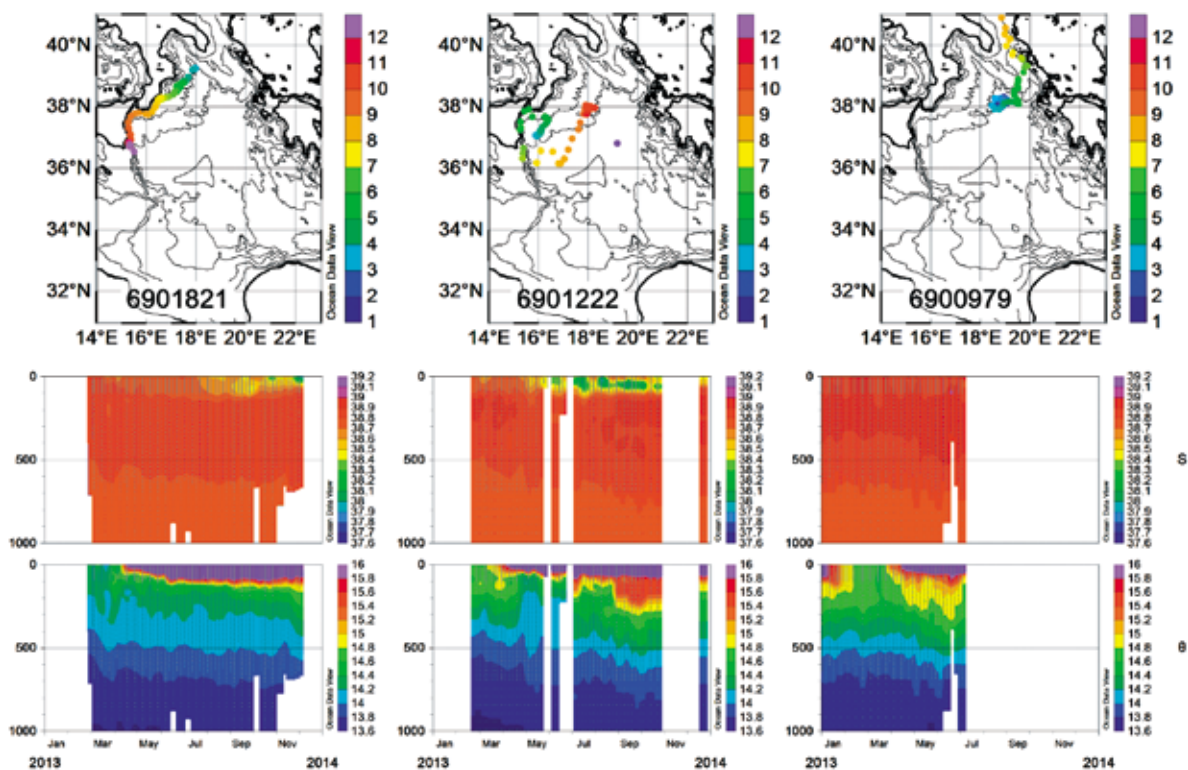


Fig. 10. Month-depth diagram depicting the time evolution of  $S$  and  $\theta$  ( $^{\circ}\text{C}$ ) from some of the profiles carried out in the northwestern (a, b) and northern (c) Ionian during 2013 in the upper 1000 m. Top: colour scale of the float trajectory indicates the month of the year

$\sim 13.60$   $^{\circ}\text{C}$ ) deep waters originating from the Levantine/Aegean Seas. There is a gradual decrease of  $S$  and  $\theta$  with depth, but the values do not drop below 38.74 and 13.50  $^{\circ}\text{C}$ , respectively. Float 6901817 (Fig. 9b) veers toward south where the deep structure is characterized by the presence of less salty and cooler waters. These waters occupy a thicker layer as approaching the bottom slope area between 33 and 34 $^{\circ}\text{N}$  along 20 $^{\circ}\text{E}$ . The pathway of float 6900843 (Fig. 9c) meanders during 2013 at 350 m depth, sampling relatively saline and warm deep waters along the eastern flank of the Ionian. As it deviates toward the centre of the basin, waters of lower  $\theta$  and  $S$  emerge from the deepest part of the basin located at the 2000 m boundary (Fig. 9c): they are likely associated with a signal of the Eastern Mediterranean Deep Water of past Adriatic origin residing at greater depths.

In the northwestern Ionian (Figs. 10a, 10b) the AW leaves its footprint both near-shore and

offshore in the upper 100 m. The near-shore sites at the perimeter corresponding to the September–November 2013 (Fig. 10a), and May–July 2013 periods (Fig. 10b) have higher salinity than the offshore region that was sampled during August–November (Fig. 10b). In general, the AW is found there, because it is transported northeastward by an anticyclonic veering in the centre of the Ionian, and by a cyclonic meander east of Sicily. This behaviour is similar to that of 2012 and this suggests a continuation in the premature reversal of the basin wide Ionian circulation, i.e. the 2012 anomalous reversal with respect to the decadal cyclonic/anticyclonic mode (GAČIĆ *et al.*, 2014). In Fig. 10c the time evolution of the thermohaline properties depicted by float 6900979 shows that along the eastern flank the upper layer salinities were high, and there was no signature of the AW.

In the region over the slope between 1000 and 2000 m isobaths on the Ionian western flank

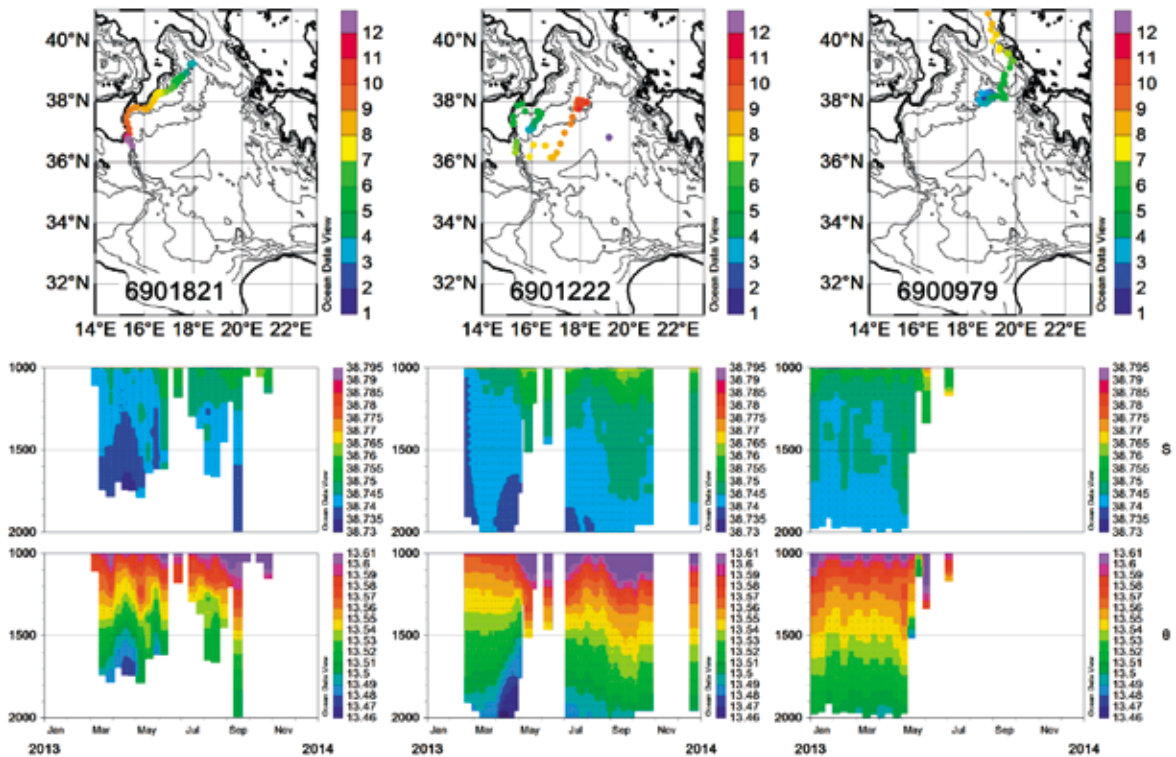


Fig. 11. Month-depth diagram depicting the time evolution of  $S$  and  $\theta$  ( $^{\circ}\text{C}$ ) from some of the profiles carried out in the northern and northwestern Ionian during 2013 in the layer between 1000 and 2000 m. Top: colour scale of the float trajectory indicates the month of the year

(Figs. 11a and 11b) we observe a clear signal of the AdDW as the relatively coolest and freshest vein about 300 m thick. It is captured by float 6901821, which crosses the area 38–39 $^{\circ}\text{N}$ , 17–18 $^{\circ}\text{E}$  during March–April 2013 (Fig. 11a). Due to the time needed for the AdDW to reach this area of the Ionian Sea (RUBINO & HANIBUCHER, 2007; BENSI *et al.* 2013b), we exclude that this signal refers to dense waters produced in the Adriatic Sea in winter 2013. Float 6901222 also captured the signal of AdDW, almost simultaneously, within the area 37–38 $^{\circ}\text{N}$ , 16 $^{\circ}\text{E}$  (Fig. 11b), where the AdDW core seems to deepen if compared with the properties in Fig. 11a. Its signal in  $S$  and  $\theta$  (both are diminishing) approaches the 2000 m horizon. We can speculate that this signal protrudes even into deeper layers, but out of reach of the float profiles. A weaker but still detectable signal of this water is present at 17 $^{\circ}\text{E}$  and as far south as 36 $^{\circ}\text{N}$ . Its footprint disappears from this layer as the float moves towards north. Float 6900979 (Fig. 11c), moves within

the area where the AdDW signal does not have the properties observed in the western part of the northern Ionian. However, it can be recognized mainly due to the  $\theta$  decrease. It appears locally and intermittently, either just at the lower boundary of the 2000 m deep layer, or near the bottom in the area shallower than 1500 m (Fig. 11c). Here the minimum observed values are not lower than 13.46  $^{\circ}\text{C}$  for  $\theta$  and 38.735 for  $S$ .

In the upper 2000 m of the northern Ionian,  $S$  and  $\theta$  values observed during 2013 are definitely higher than the AdDW signature in 2012 in that area. This can be explained by the lack of the AdDW with the same characteristics as in 2012. In the meantime this 2012 AdDW spread and probably sank to greater depths, possibly displacing older AdDW, which appears as intrusion from the deep layers ( $> 2000$  m) into the layer 1000–2000 m, as we also observed during the oceanographic campaign ADREX-2014 (PERSEUS project) conducted in February 2014 (not shown here).

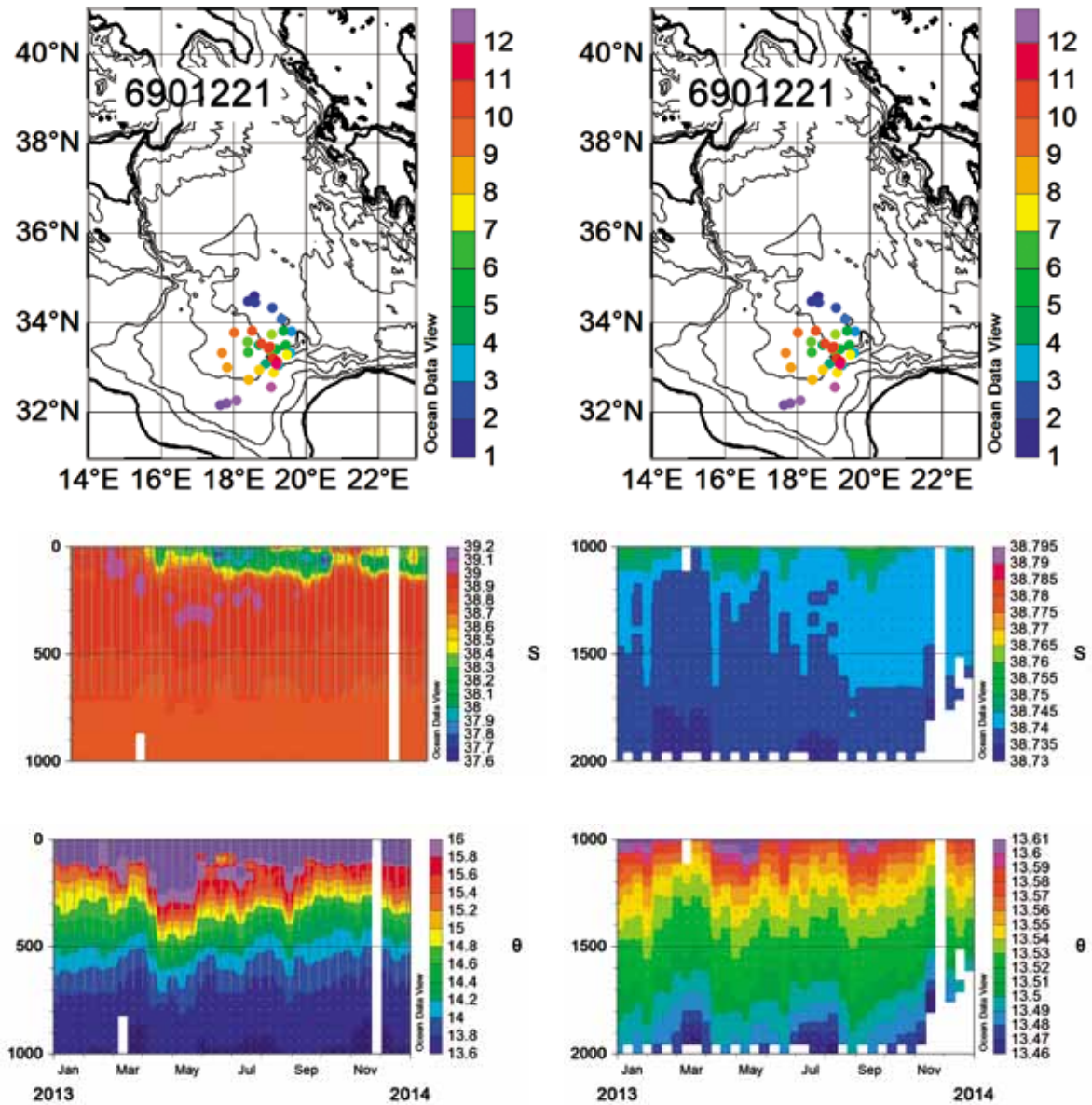


Fig. 12. Month-depth diagram depicting the time evolution of  $S$  and  $\theta$  ( $^{\circ}\text{C}$ ) from one float in the southern Ionian during 2013 in the (a) upper 1000 m and (b) between 1000 and 2000 m. Out-of scale values for  $\theta$  in a) are comprised in the interval [18.6, 28]. Top: colour scale of the float trajectory indicates the month of the year

In the southern Ionian (Fig. 12a) the AW is mostly detected within the 33 - 34°N, 18 - 20°E, as a subsurface salinity minimum. Other two floats (not shown), one to the east and one to the west from the one we illustrate in Fig. 12a, have similar characteristics regarding the AW. Ultimately, it seems that the AW that enters through the Sicily Channel, splits into two branches south of Sicily, one of them follows a path toward the northern Ionian while the other

travels directly towards the Levantine basin, as also reported by BESSIERES *et al.* (2013).

At the southern Ionian periphery (Fig. 12b), as soon as the float reaches the slope boundary between 1000 and 2000 m isobaths, a clear signal of the AdDW appears as a relative  $S$  and  $\theta$  minimum. The lowest values detected are  $< 13.46$   $^{\circ}\text{C}$  for  $\theta$ , and  $< 38.735$  for  $S$ . This AdDW is different from that observed in the north-western Ionian (Figs. 11a, 11b). Some recent studies,

(such as in RUBINO & HAINBUCHER, 2007; CARDIN *et al.*, 2011; BENSI *et al.*, 2013a) established the decadal variability of the Adriatic dense water production and DWO discharge from the Adriatic into the Ionian. Therefore, what we observe in the southern part of the Ionian, might be the remnant of the AdDW formed and spread in the '90 or even before the EMT (SPARNOCCHIA *et al.*, 2011; BENSI *et al.*, 2013b). The present profiles do not reach more than 2000 m, and therefore we are not able to describe the properties beneath this depth. We, nevertheless, observe that the AdDW discharged during the past times likely influences the periphery of the Ionian Sea. It possibly resided at greater depths, and was sporadically lifted up due to the change of the circulation mode. During the EMT, in the eastern and central part of the Ionian, its displacement was due to the DWO from the Aegean Sea (ROETHER *et al.*, 2007), but as the DWO from the Aegean ceased, AdDW overtook its role of principal contributor for the Eastern Mediterranean Deep Water, which is able to displace (when dense enough) the older AdDW.

## CONCLUSIONS

The surface geostrophic flow from altimetry data, as well as the 350 m and 1000 m depth circulation reconstructed from Lagrangian measurements, give evidence of the principal dynamic structures. They consist of very energetic eddies and gyres at spatial scales of about 100 km. Already known from previous studies, the presence of Pelops Gyre is documented for the entire study period extending vertically over the water column from the surface to 1000 m depth. In addition, a recurrent anticyclonic gyre located in the centre of the Ionian basin over the major depression (~4600 m depth) near the northern border of the MIJ was evidenced as a very prominent feature. This gyre also extends from surface to 1000 m depth. The basin-wide mean circulation can hardly be detected. Some evidence of it is observed only in the close vicinity of both eastern and western Ionian flanks. Float data suggest that in the northernmost

portion of the Ionian the sub-basin circulation is prevalently cyclonic, in agreement with the surface geostrophic flow pattern from altimetry data. The spreading over the Ionian area and mixing of the Levantine Intermediate Water are influenced by the dynamic structures. In the northern part, they are also influenced by the exchange through the Strait of Otranto, as shown from the S example. The DWO from the Southern Adriatic in 2012 has left a clear signal in the northern Ionian, where the available profiles indicated that spreading occurs along and across the deep isobaths (1500, 2000 m) circulating along the slope in the cyclonic sense. This signal loses strength, or, which is even more probable, sinks at depths greater than 2000 m in 2013. If so, this recent dense water is about to modify the deep layer properties, which will have probable future impact on the deep layers both along the periphery and in the central portion of the Ionian Sea. Thus, the East Mediterranean Deep Water, is about to continue modifying its thermohaline properties, and eventually export them into the deep Levantine basin.

## ACKNOWLEDGEMENTS

The Argo float data were collected and made freely available by the Coriolis Global Data Assembly Centers (GDAC) (<http://www.coriolis.eu.org>).

The altimeter products (ADT) were produced by Ssalto/Duacs and distributed by Aviso, with support from Cnes (<http://www.aviso.oceanobs.com/duacs/>).

Partial support from the national projects RITMARE (La Ricerca Italiana per il MARE, Programma Nazionale di Ricerca Scientifica e Tecnologica), Argo-Italy and the MedGES (Mediterranean Good Environmental Status) is greatly acknowledged.

PERSEUS Project (<http://www.perseus-net.eu>) is granted for the possibility to consult the data collected during the ADREX-2014 cruise in February 2014.

Most of the figures were produced by Ocean Data View (SCHLITZER, 2015).

## REFERENCES

- ARGO QUALITY CONTROL MANUAL. 2013. Version 2.8, 3 January 2013, Argo Data Management. [Available at <http://www.argodatamgt.org/content/download/15699/102401/file/argo-quality-control-manual-version2.8.pdf>].
- BENSI, M., V. CARDIN, A. RUBINO, G. NOTARSTEFANO & P.-M. POULAIN. 2013a. Effects of winter convection on the deep layer of the Southern Adriatic Sea in 2012. *J. Geophys. Res. Oceans*, 118: 6064–6075, doi:10.1002/2013JC009432.
- BENSI, M., A. RUBINO, V. CARDIN, D. HAINBUCHER & I. MANCERO-MOSQUERA. 2013b. Structure and variability of the abyssal water masses in the Ionian Sea in the period 2003-2010. *J. Geophys. Res. Oceans*, 118, doi:10.1029/2012JC008178.
- BESSIERES, L., M.H. RIO, C. DUFAU, C. BOONE & M.I. PUJOL. 2013. Ocean state indicators from MyOcean altimeter products. *Ocean Sci.*, 9: 545–560.
- CARDIN, V., M. BENSI & M. PACCIARONI. 2011. Variability of water mass properties in the last two decades in the Southern Adriatic Sea with emphasis on the period 2006-2009. *Continental Shelf Research*, 31 (9): 951–965.
- EMERY, W.J., W.G. LEE, & L. MAGAARD. 1984. Geographic and Seasonal Distribution of Brunt-Väisälä Frequency and Rossby Radii in the North Pacific and North Atlantic. *J. Phys. Oceanogr.*, 14., 294-317.
- GAČIĆ, M., G.L. EUSEBI BORZELLI, G. CIVITARESE, V. CARDIN, & S. YARI. 2010. Can internal processes sustain reversals of the ocean upper circulation? The Ionian Sea example. *Geophysical Research Letters*, 37, L09608, doi:10.1029/2010GL043216.
- GAČIĆ, M., G. CIVITARESE, G. L. E. BORZELLI, V. KOVAČEVIĆ, P.-M. POULAIN, A. THEOCHARIS, M. MENNA, A. CATUCCI & N. ZAROKANELLOS. 2011. On the relationship between the decadal oscillations of the northern Ionian Sea and the salinity distributions in the eastern Mediterranean, *J. Geophys. Res.*, 116, C12002, doi:10.1029/2011JC007280.
- GAČIĆ, M., K. SCHROEDER, G. CIVITARESE, S. COSOLI, A. VETRANO & G. L. EUSEBI BORZELLI. 2013. Salinity in the Sicily Channel corroborates the role of the Adriatic–Ionian Bimodal Oscillating System (BiOS) in shaping the decadal variability of the Mediterranean overturning circulation. *Ocean Sci.*, 9: 83–90. doi:10.5194/os-9-83-2013.
- GAČIĆ, M., G. CIVITARESE, V. KOVAČEVIĆ, L. URSELLA, M. BENSI, M. MENNA, V. CARDIN, P.-M. POULAIN, S. COSOLI, G. NOTARSTEFANO & C. PIZZI. 2014. Extreme winter 2012 in the Adriatic: an example of climatic effect on the BiOS rhythm. *Ocean Sci.*, 10, 513-522, 2014 doi:10.5194/os-10-513-2014.
- GRILLI, F. & N. PINARDI. 1998. The computation of Rossby radii of deformation for the Mediterranean Sea. *MTP news* 6 (4).
- HAMAD, N., C. MILLOT & I. TAUPIER-LETAGE. 2006. The surface circulation in the eastern basin of Mediterranean Sea. *Sci. Mar.*, 70(3): 457-503.
- LARNICOL, G., N. AYOUB & P.Y. LE TRAON. 2002. Major changes in Mediterranean Sea level variability from 7 years of TOPEX/Poseidon and ERS-1/2 data. *J. Mar. Syst.*, 33 – 34: 63–89, doi:10.1016/S0924-7963(02)00053-2.
- MALANOTTE-RIZZOLI, P., B.B. MANCA, M. RIBERA D'ALCALÀ, A. THEOCHARIS, A. BERGAMASCO, D. BREGANT, G. BUDILLON, G. CIVITARESE, D. GEORGOPOULOS, A. MICHELATO, E. SANSONE, P. SCARAZZATO, E. SOUVERMEZOGLOU. 1997. A synthesis of the Ionian Sea hydrography, circulation and water mass pathways during POEM-Phase I. *Prog. Oceanog.* 39, 153-204., doi:10.1016/S0079-6611(97)00013-X.
- MENNA, M. & P.-M. POULAIN. 2010. Mediterranean intermediate circulation estimated from Argo data in 2003-2010. *Ocean Science*, 6: 331-343.
- MIHANOVIĆ, H., I. VILIBIĆ, S. CARNIEL, M. TUDOR, A. RUSSO, A. BERGAMASCO, N. BUBIĆ, Z. LJUBEŠIĆ, D. VILIČIĆ, A. BOLDRIN, V. MALAČIĆ, M. CELIO, C. COMICI & F. RAICICH. 2013. Exceptional dense water formation on the Adriatic shelf in the winter of 2012. *Ocean Sci.*, 9: 561-572, doi:10.5194/



- os-9-561-2013. [Available at [www.ocean-sci.net/9/561/2013/](http://www.ocean-sci.net/9/561/2013/)].
- MILLOT, C. & I. TAUPIER-LETAGE. 2005. Circulation in the Mediterranean Sea. *Handb. Environ. Chem.* 5(K): 29-66.
- NITTIS, K., N. PINARDI, A. LASCARATOS. 1993. Characteristics of the Summer 1987 Flow Field in the Ionian Sea. *J. Geophys. Res.*, 98, C6, 10,171-10,184.
- NOTARSTEFANO, G. & P.-M. POULAIN. 2008. Delayed mode quality control of Argo floats salinity data in the Tyrrhenian Sea. *Rel. 2008/125 OGA 43 SIRE*, Trieste, Italy, 33 pp.
- NOTARSTEFANO, G. & P.-M. POULAIN. 2013. Delayed mode quality control correction for a salinity offset of Argo float WMO 6900952 in the Mediterranean Sea. *Rel. 2013/35 Sez. OCE 18 MAOS*.
- OWENS, W.B., & A.P.S. WONG. 2009. An improved calibration method for the drift of the conductivity sensor on autonomous CTD profiling floats by  $\theta$ -S climatology. *Deep Sea Res. Part I: Oceanographic Research Papers*, 56(3): 450-457.
- POULAIN, P.-M., R. BARBANTI, J. FONT, A. CRUZADO, C. MILLOT, I. GERTMAN, A. GRIFFA, A. MOLCARD, V. RUPOLO, S. LE BRAS & L. PETIT DE LA VILLEON. 2007. MedArgo: a drifting profiler program in the Mediterranean Sea. *Ocean Sci.*, 3: 379-395.
- RIO, M.-H., P.-M. POULAIN, A. PASCUAL, E. MAURI, G. LARNICOL & R. SANTOLERI. 2007. A Mean Dynamic Topography of the Mediterranean Sea computed from altimetric data, in-situ measurements and a general circulation model. *J. Mar. Syst.*, 65: 484-508. doi:10.1016/j.jmarsys.2005.02.006.
- ROBINSON, A.R., M. GOLNARAGHI, W.G. LESLIE, A. ARTEGIANI, A. HECHT, E. LAZZONI, A. MICHELATO, E. SANSONE, A. THEOCHARIS & Ü. ÜNLÜATA. 1991. The eastern Mediterranean general circulation: features, structure and variability. *Dyn. Atmos. Oceans*, 15, 215-240.
- ROBINSON, A.R., W.G. LESLIE, A. THEOCHARIS & A. LASCARATOS. 2001. Mediterranean Sea Circulation. *Encyclopedia of Ocean Sciences*, Academic Press, 1689-1706.
- ROETHER, W., B. KLEIN, B.B. MANCA, A. THEOCHARIS, & S. KIOROGLU. 2007. Transient Eastern Mediterranean deep waters in response to the massive dense-water output of the Aegean Sea in the 1990s. *Prog. Oceanog.*, 74: 540-571.
- RUBINO, A. & D. HAINBUCHER. 2007. A large abrupt change in the abyssal water masses of the Eastern Mediterranean. *Geophys. Res. Lett.*, 34, L23607, doi:10.1029/2007GL031737.
- SCHLITZER, R., 2015. Ocean Data View, <http://odv.awi.de>.
- SPARNOCCHIA, S., G.P. GASPARINI, K. SCHROEDER & M. BORGHINI. 2011. Oceanographic conditions in the NEMO region during the KM3NeT project (April 2006-May 2009). *Nucl. Instrum. Methods Phys. Res. A*, Volumes 626-627, Supplement 1:S87-S90, ISSN 0168-9002, doi: 10.1016/j.nima.2010.06.231
- URSELLA, L., V. KOVAČEVIĆ & M. GAČIĆ. 2011. Footprints of mesoscale eddy passages in the Strait of Otranto (Adriatic Sea). *J. Geophys. Res.*, 116, C04005, doi:10.1029/2010JC006633.
- VIGO, I., D. GARCIA & B.F. CHAO. 2005. Change of sea level trend in the Mediterranean and Black seas. *J. Mar. Res.*, 63: 1085-1100. doi:10.1357/002224005775247607.

## O termohalnim svojstvima i cirkulaciji Jonskog mora u toku 2010.-2013. na osnovi mjerenja Argo plutačama

Vedrana KOVAČEVIĆ\*, Laura URSELLA, Miroslav GAČIĆ, Giulio NOTARSTEFANO, Milena MENNA, Manuel BENSI i Pierre-Marie POULAIN

*OGS (Nacionalni institut za oceanografiju i eksperimentalnu geofiziku), Borgo Grotta Gigante 42/c, Sgonico, Italija*

*\*Kontakt adresa e-mail: [vkovacevic@ogs.trieste.it](mailto:vkovacevic@ogs.trieste.it)*

### SAŽETAK

Na temelju raspoloživih podataka sistema Argo sonde i podataka o visini morske razine, analizirani su površinski, intermedijarni (350 m) i duboki (1000 m) sustavi strujanja u Jonskom moru u toku 2010., 2011., 2012. i 2013. godine. Pritom su opisana i uspoređena termohalina svojstva dobivena iz profila Argo sonde. Razmatrano je i širenje guste vode iz Jadranskog mora, naročito ono vezano uz iznimno velik gubitak topline s površine mora u toku zimskog razdoblja u 2012. godini. Tokom perioda istraživanja, polja strujanja karakteriziraju vrtlozi čiji je promjer otprilike 100 km. Vrtlog Pelops, posebice, opaža se od morske površine do 1000 m dubine. Anticiklonalna struktura u središtu Jonskog mora, na sjevernoj strani struje tzv. *Mid-Ionian Jet*, sastavljena je od više manjih vrtloga i također se proteže do istih dubina. Ciklonalno strujanje dobro se uočava na sve tri razine u rubnom (dužobalnom) području unutar sjevernog Jonskog more. Vrlo izrazit signal prisustva guste jadranske vode (*Adriatic Dense Water, AdDW*) opažen je na otprilike 1000 m dubine u sjeverozapadnom dijelu jonskog bazena u kasno proljeće 2012. godine. Otuda, AdDW vrlo vjerojatno postupno tone struajući prema jugu, i njen se signal više ne opaža jer su Argo mjerenja ograničena na maksimalnu dubinu od 2000 m.

**Ključne riječi:** Jonsko more, uzgonske plutače, površinska topografija, prostorna varijabilnost na skali *sub-basin*, višegodišnja promjenjivost